Reversible and Irreversible Potentials and an Inaccuracy in Popular Models in the Fuel Cell Literature

Uday K. Chakraborty

Department of Mathematics and Computer Science, University of Missouri, St. Louis, MO 63121, USA;
chakrabortyu@umsl.edu

check for
updates

Abstract: Modeling is an integral part of fuel cell design and development. This paper identifies a long-standing inaccuracy in the fuel cell modeling literature. Specifically, it discusses an inexact insertion, in popular models, of cell/stack current into Nernst's equation in the derivation of output (load) voltage. The origin of the inaccuracy is traced to the nature of reversible and irreversible potentials (equilibrium and non-equilibrium states) in the cell. The significance of the inaccuracy is explained in the context of the electrochemistry and thermodynamics of the fuel cell.

Keywords: fuel cell model; fuel cell stack; hydrogen; Nernst equation; proton exchange membrane fuel cell (PEMFC); solid oxide fuel cell (SOFC)

1. Introduction

Modeling the operation of fuel cells is an indispensable part of fuel cell research. In many papers in the literature involving the modeling of solid oxide fuel cells (SOFCs) and proton exchange membrane fuel cells (PEMFCs), an inaccuracy is found in the cell/stack voltage expression (see, for example, references [1–30]). We argue that the problem arises because of an inexact intermediate step in the derivation of the output voltage. The origin of this inaccuracy can be traced to the substitution in the Nernst equation of activity (or concentration or partial pressure) with a function of the load current. An analysis of the flaw is presented in the remainder of this paper.

2. Background: The Nernst Equation

The Nernst equation, which is the cornerstone of fuel cell thermodynamics, provides an expression for the reversible thermodynamic potential, also known as the equilibrium voltage or the open-circuit electromotive force (EMF), of the fuel cell [31]:

$$E_{Nernst} = E_0 + \frac{RT}{nF} \ln \left(\frac{\prod_i a_{reactant_i}^{c_i}}{\prod_j a_{product_j}^{c_j}} \right) \tag{1}$$

where E_0 is the reference (standard) EMF at unit activity and atmospheric pressure; i and j are the numbers of reactant and product species; a represents the *activity*; c_i is the stoichiometric coefficient of species i; R is the universal gas constant; F is Faraday's constant; n is the number of electrons transferred for each molecule of the fuel participating in the reaction; and T is the temperature. For a hydrogen–oxygen fuel cell (e.g., solid oxide fuel cell or proton exchange membrane fuel cell), hydrogen and oxygen are the reactants, and the product is water (or steam). The reference EMF, E_0, depends on the temperature, T:

$$E_0 = E_0^0 + (T - T_0)\frac{\Delta s}{nF}, \tag{2}$$

where E_0^0 is the standard EMF at temperature T_0, and Δs is the change in entropy. The activity, a, of an ideal gas is expressed in terms of its pressure (or partial pressure), p:

$$a_{H_2} = \frac{p_{H_2}}{p^0}, \tag{3}$$

$$a_{O_2} = \frac{p_{O_2}}{p^0}, \tag{4}$$

where p^0 is the standard-state pressure (1 atm). At high temperatures, such as 1000 °C (as in solid oxide fuel cells), steam can be assumed to behave as an ideal gas, and therefore,

$$a_{H_2O} = \frac{p_{H_2O}}{p^0}. \tag{5}$$

Using $p^0 = 1$ atm, and noting that $n = 2$ for a hydrogen fuel cell, we have the following version of the Nernst equation for solid oxide fuel cells:

$$E_{Nernst} = E_0 + \frac{RT}{2F} \ln \left(\frac{p_{H_2} \sqrt{p_{O_2}}}{p_{H_2O}} \right). \tag{6}$$

If the fuel cell is operated below 100 °C so that liquid water is produced (as in proton exchange membrane fuel cells), the activity of water can be taken to be unity ($a_{H_2O} = 1$). In that case, the Nernst equation takes the form

$$E_{Nernst} = E_0 + \frac{RT}{2F} \ln \left(p_{H_2} \sqrt{p_{O_2}} \right). \tag{7}$$

3. The Inaccuracy in the Model

Drawing inspiration from the pioneering work in reference [1] where an elegant dynamic model for an SOFC plant was developed, many later papers (e.g., references [2–30]) re-derived and/or built upon the model, expressing the partial pressures of the reactants and products as functions of the cell current (not to be confused with the exchange current [31] or the fuel crossover/internal current [31]), before inserting those partial pressure expressions into the Nernst equation.

Reference [1], in its "dynamic behaviour algorithm" (Figure 2 on p. 497 of that paper), expressed (i) the partial pressures of the reactants and products in terms of the corresponding molar flow rates, and (ii) the molar flow rates taking part in the reaction in terms of cell (load) current, and inserted the resulting expressions of p_{H_2}, p_{O_2} and p_{H_2O} into Equation (6).

Building upon reference [1], other papers (e.g., references [6,7,12,14–16,19,20]) obtained essentially the same core model with the following fallacious form of the Nernst equation:

$$E_{Nernst} = E_0 + \frac{RT}{2F} \left\{ \ln \left(\frac{K_{H_2O}}{K_{H_2}} \sqrt{\frac{K_r}{r_{HO} K_{O_2}}} \right) + \frac{1}{2} \ln \left(I_{FC} \left(\frac{1}{u} - 1 \right)^2 \left(\frac{2}{u} - r_{HO} \right) \right) \right\}, \tag{8}$$

where K_{H_2}, K_{O_2}, and K_{H_2O} are valve molar constants [1]; $K_r = 1/(4F)$ [1,12,13]; r_{HO} is the ratio of the input molar flow rates of hydrogen and oxygen [2,6]; u is the fuel utilization ratio [2,6]; and I_{FC} is the load current [6]. A detailed derivation of Equation (8) is given in the following sub-section.

Derivation of the Fallacious Expression

A derivation of the fallacious form of the Nernst voltage expression (Equation (8)) is presented here. This derivation follows the treatment in references [1,6,12]. A single cell is considered here; the extension of the derivation to a stack is trivially easy.

Assuming perfect gas properties for hydrogen at the anode channel, we have

$$p_{H_2}^{anode} V_{anode} = n_{H_2}^{anode} RT, \tag{9}$$

where $p_{H_2}^{anode} = p_{H_2}^{anode}(t)$ is the partial pressure of hydrogen in the anode channel; $n_{H_2}^{anode} = n_{H_2}^{anode}(t)$ is the number of moles of hydrogen in the anode channel; and V_{anode} is the anode volume. Taking the derivative with respect to time, we can express the rate of change of partial pressure in terms of the molar flow rate:

$$\frac{d}{dt} p_{H_2}^{anode}(t) = \frac{RT}{V_{anode}} \left(q_{H_2}^{anode}(t) \right), \tag{10}$$

with $q_{H_2}^{anode}(t)$ defined as

$$q_{H_2}^{anode}(t) = \frac{d}{dt} n_{H_2}^{anode}(t). \tag{11}$$

Splitting $q_{H_2}^{anode}(t)$ into its three components, namely, the input flow rate, the flow rate that takes part in the reaction, and the output flow rate, we have

$$q_{H_2}^{anode}(t) = q_{H_2}^{in}(t) - q_{H_2}^{react}(t) - q_{H_2}^{out}(t), \tag{12}$$

and thus (omitting the t for simplicity)

$$\frac{d}{dt} p_{H_2}^{anode} = \frac{RT}{V_{anode}} \left(q_{H_2}^{in} - q_{H_2}^{react} - q_{H_2}^{out} \right). \tag{13}$$

The process of oxygen inflow–reaction–outflow at the cathode channel can be described by

$$\frac{d}{dt} p_{O_2}^{cathode} = \frac{RT}{V_{cathode}} \left(q_{O_2}^{in} - q_{O_2}^{react} - q_{O_2}^{out} \right). \tag{14}$$

In SOFCs, water vapor (steam) forms at the anode:

$$\frac{d}{dt} p_{H_2O}^{anode} = \frac{RT}{V_{anode}} \left(0 + q_{H_2O}^{react} - q_{H_2O}^{out} \right). \tag{15}$$

In PEMFCs, water forms at the cathode. Of course, when liquid water is produced in a fuel cell (as in PEMFCs), we have

$$p_{H_2O} = 1. \tag{16}$$

Assuming that "the molar flow of any gas through the valve is proportional to its partial pressure inside the channel" [1], we have for an SOFC

$$\frac{q_{H_2}^{out}}{p_{H_2}} = K_{H_2} \tag{17}$$

and

$$\frac{q_{H_2O}^{out}}{p_{H_2O}} = K_{H_2O} \tag{18}$$

at the anode and

$$\frac{q_{O_2}^{out}}{p_{O_2}} = K_{O_2} \tag{19}$$

at the cathode, with K_{H_2}, K_{H_2O}, and K_{O_2} being constants.

From electrochemistry we know that

$$q_{H_2}^{react} = q_{H_2O}^{react} = 2q_{O_2}^{react} = \frac{I_{FC}}{2F}, \tag{20}$$

where $I_{FC} = I_{FC}(t)$ is the cell current. Upon the introduction of a constant [1,13],

$$K_r = \frac{1}{4F},\tag{21}$$

Equation (20) yields

$$q_{H_2}^{react} = q_{H_2O}^{react} = 2K_r I_{FC}\tag{22}$$

and

$$q_{O_2}^{react} = K_r I_{FC}.\tag{23}$$

Now, inserting Equations (17) and (22) into Equation (13) and taking the Laplace transform (we use the notation that the transform of $x(t)$ is $\mathcal{X}(s)$), we get [12]

$$s\mathcal{P}_{H_2}(s) - p_{H_2}(0) = \frac{RT}{V_{anode}}\left(\mathcal{Q}_{H_2}^{in}(s) - 2K_r\mathcal{I}_{FC}(s) - K_{H_2}\mathcal{P}_{H_2}(s)\right)\tag{24}$$

which, upon the substitution of $p_{H_2}(0) = 0$ and

$$\tau_{H_2} = \frac{V_{anode}}{K_{H_2}RT},\tag{25}$$

becomes

$$\mathcal{P}_{H_2}(s) = \frac{1/K_{H_2}}{1 + \tau_{H_2}s}\left(\mathcal{Q}_{H_2}^{in}(s) - 2K_r\mathcal{I}_{FC}(s)\right).\tag{26}$$

Similarly, for oxygen, Equations (14), (19) and (23) yield

$$s\mathcal{P}_{O_2}(s) - p_{O_2}(0) = \frac{RT}{V_{cathode}}\left(\mathcal{Q}_{O_2}^{in}(s) - K_r\mathcal{I}_{FC}(s) - K_{O_2}\mathcal{P}_{O_2}(s)\right)\tag{27}$$

which, with the substitution of $p_{O_2}(0) = 0$ and

$$\tau_{O_2} = \frac{V_{cathode}}{K_{O_2}RT},\tag{28}$$

gives

$$\mathcal{P}_{O_2}(s) = \frac{1/K_{O_2}}{1 + \tau_{O_2}s}\left(\mathcal{Q}_{O_2}^{in}(s) - K_r\mathcal{I}_{FC}(s)\right).\tag{29}$$

Finally, for steam, we have from Equations (15), (18), and (22)

$$\mathcal{P}_{H_2O}(s) = \frac{1/K_{H_2O}}{1 + \tau_{H_2O}s}2K_r\mathcal{I}_{FC}(s)\tag{30}$$

where

$$\tau_{H_2O} = \frac{V_{anode}}{K_{H_2O}RT}.\tag{31}$$

(Equations (26), (29) and (30) were used in Figure 2 of reference [1].)

Now, applying the inverse Laplace transform to Equation (26) allows us go from the *s*-domain back to the time domain:

$$p_{H_2}(t) = \frac{1}{K_{H_2}\tau_{H_2}}exp\left(\frac{-t}{\tau_{H_2}}\right)\int_{\theta=0}^{t}\left(q_{H_2}^{in}(\theta) - 2K_r I_{FC}(\theta)\right)exp\left(\frac{\theta}{\tau_{H_2}}\right)d\theta.\tag{32}$$

The steady-state partial pressure, then, is obtained from the above equation as

$$p_{H_2,ss} = \frac{1}{K_{H_2}}\left(q_{H_2,ss}^{in} - 2K_r I_{FC,ss}\right).\tag{33}$$

(A simpler derivation of Equation (33) is given in Appendix A.1) The steady-state partial pressures of oxygen and steam are obtained similarly:

$$p_{O_2,ss} = \frac{1}{K_{O_2}} \left(q_{O_2,ss}^{in} - K_r I_{FC,ss} \right) \tag{34}$$

and

$$p_{H_2O,ss} = \frac{1}{K_{H_2O}} 2 K_r I_{FC,ss}. \tag{35}$$

Now, plugging the above three Equations (33)–(35), as well as the definitions of u and r_{HO} (Equations (A4) and (A5), respectively, from Appendix A.2) into the Nernst EMF expression (Equation (6) of Section 2), we obtain, after some algebra (see Appendix A.2), our familiar Equation (8).

4. Analysis of the Inaccuracy

The terminal (load) voltage is generally obtained by subtracting the following types of losses (or "irreversibilities") from E_{Nernst}:

- activation loss;
- concentration loss;
- ohmic loss; and
- losses due to fuel crossover and internal current.

Equation (8), or one of its many (implicit or explicit) variants, has been the mainstay of a line of fuel cell modeling research for about two decades now (examples abound; a few representative articles are listed in the References section). Not all of the models in references [1–30] show the explicit form of Equation (8), but they all use some form of this equation, by expressing—directly or indirectly—the Nernst voltage as a function of, among other variables, current.

The problem with Equation (8) is that it mixes equilibrium and non-equilibrium expressions. The Nernst voltage (EMF) is the *reversible* thermodynamic potential that applies only to the *equilibrium* condition of the cell; the equilibrium is lost when current is drawn from the cell. In other words, the Nernst voltage is, by definition, the open-circuit EMF and cannot therefore be expressed in terms of the cell (load) current or current density.

That the use of I_{FC} in Equation (8) is questionable can also be seen from the fact that setting

$$I_{FC} = 0$$

causes the right side to be mathematically undefined.

The effect of Equation (8) on the output voltage can be seen in the SOFC polarization curve (Figure 1) obtained from the following relationship:

$$V = E_{Nernst} - r I_{FC}, \tag{36}$$

where V is the output (load) voltage; E_{Nernst} is given by Equation (8); and r is the ohmic resistance of the cell (cell parameter values, taken from references [1,6,12], are given in Table 1). The upper curve (red) in Figure 1 shows the Nernst voltage, E_{Nernst}, computed from Equation (8), while the lower one plots the output voltage, V. Equation (36), like Equation (12) of reference [1] and Equation (6) of reference [6], considers only the ohmic loss out of the four types of losses mentioned earlier.

Table 1. Numerical values of parameters and constants.

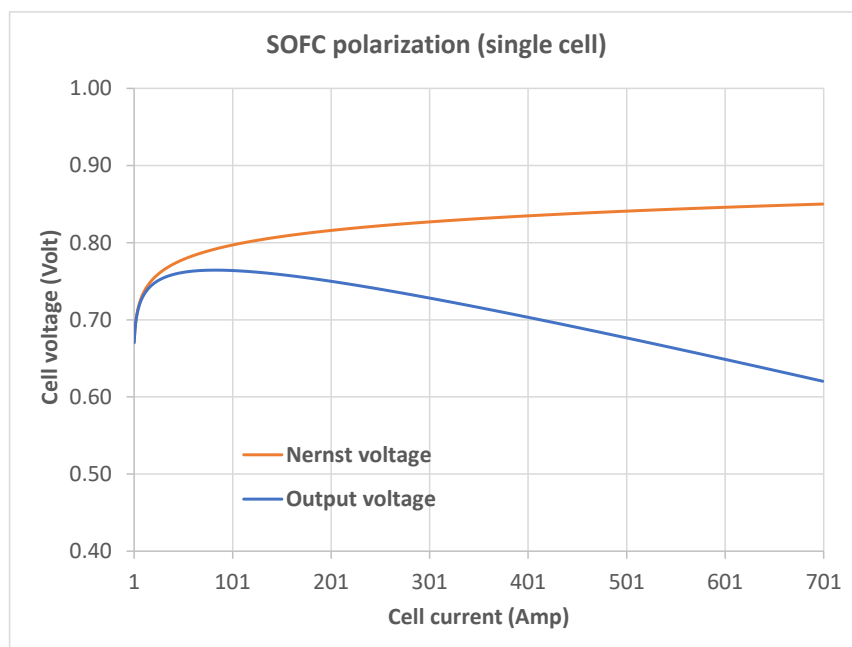| Parameter	Value
T	1273 K
E_0	1.18 V
u	0.8
K_r	$1/(4F)$ mol/(s.A)
K_{H_2}	0.843 mol/(s.atm)
K_{H_2O}	0.281 mol/(s.atm)
K_{O_2}	2.52 mol/(s.atm)
r	3.28125×10^{-4} Ω
r_{HO}	1.145
n	2
Constants	
F	96,485 Coulombs/mol
R	8.31 J/(mol K)

Figure 1. Solid oxide fuel cell (SOFC) polarization obtained with E_{Nernst} given by Equation (8).

Figure 1 has the horizontal (current) axis starting at 1 A, not zero, because in Equation (8), the Nernst voltage is undefined at $I_{FC} = 0$.

Figure 1 shows an increase in the Nernst voltage with an increasing load current. At first sight, it may not be immediately clear how the model represented by Equation (8) produces the *V*-values in this figure (it may not be impossible for the polarization characteristics in Figure 1 to be obtained from actual measurements of a physical fuel cell stack under specific operating conditions; much depends on fuel flow, fuel utilization, thermal effects, diffusion, back-diffusion, load current and voltage requirements, and not all complex interactions are fully understood). It can, however, be argued that Equation (8) produces this polarization curve by holding both u and r_{HO} constant to mimic a constant fuel utilization ratio and a constant hydrogen–oxygen ratio of input flow rates. We need to account for the changes in the *V*-values without having to make E_{Nernst} a function of current.

For a head-to-head comparison of the polarization produced by Equation (8) with the "correct" polarization, we need the "correct" Nernst voltage (that is, the Nernst voltage at open circuit), which,

unfortunately, cannot be obtained from Equation (8). (We could, of course, obtain the correct Nernst voltage by assuming reasonable values for p_{H_2}, p_{O_2} and p_{H_2O} and plugging those values, along with the relevant parameter values from Table 1, into Equation (6), but the resulting Nernst voltage would have no connection to Equation (8).) We circumvent this difficulty by extrapolating the open-circuit Nernst voltage from values produced by Equation (8). Specifically, we use a trivial extrapolation where we obtain the point where the line joining the first two points—(1 A, 0.670472 V) and (2 A, 0.689471 V)—meets the I_{FC} = 0 line. This gives us an extrapolated

$$E_{Nernst} = 0.651473 \text{ V},$$

which is used in Figure 2 to show the "correct" polarization behavior. The upper plot (red) in Figure 2 represents the (constant) Nernst voltage, and the lower one shows the output values from Equation (36) (obviously, both the plots in this figure are straight lines). For ease of comparison with Figure 1, the current axis in Figure 2 starts from 1 A.
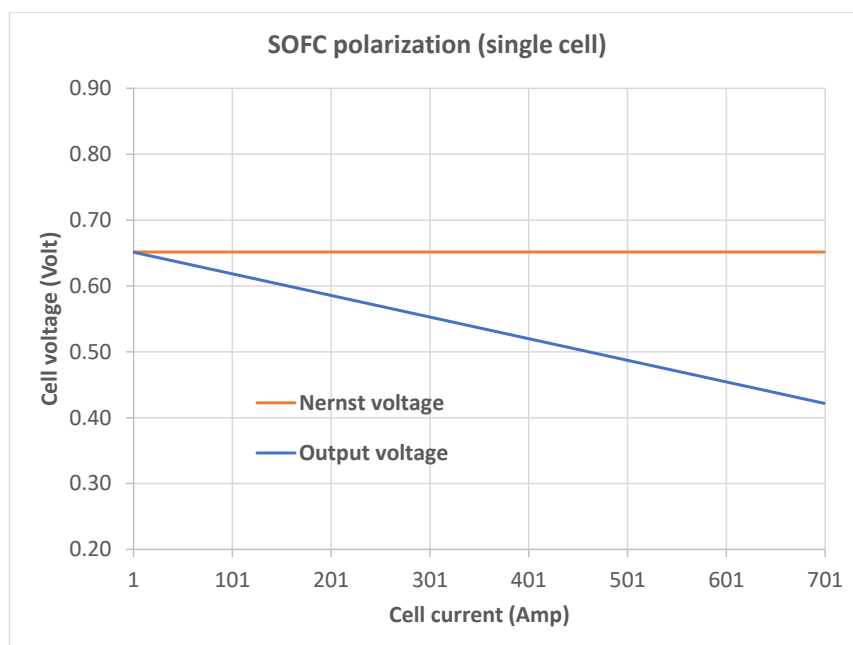

Figure 2. SOFC polarization obtained with E_{Nernst} = 0.651473 V.

5. Discussion

If a non-zero current is to be considered, the proper equation to use is the Butler–Volmer equation, not the Nernst equation. The current–voltage relationship at a non-zero current (away from equilibrium) is perhaps best investigated using reaction kinetic expressions with microscopic reversibility. When modeling specific polarization behaviors, it is important to distinguish between the "reversible" potential and the "irreversibilities".

The difference between reversible and irreversible potentials and its connection to the Nernst equation are important in the study of solid oxide electrolysis cells (e.g., [32]), too.

In reference [33], the partial pressures of hydrogen and oxygen of a proton exchange membrane fuel cell are expressed (in Equations (2) and (3) of that paper [33]) in terms of current, but before these partial pressures are plugged into the Nernst equation Equation (1) of that paper [33]) to obtain the reversible potential, the current, correctly, is set to zero. Reference [33] also reported using non-zero values of current in the Nernst equation.

Reference [12] used Equation (8) to generate both training and test data, and therefore, none of the conclusions in that paper are invalidated by the inaccuracy discussed here.

6. Conclusions

An inaccuracy in the fuel cell modeling literature involving the nature of the reversible thermodynamic potential was identified in this paper. An analysis of the inaccuracy was provided and its significance explained. To summarize, there is nothing wrong with the Nernst equation that provides the reversible (equilibrium) voltage of a fuel cell; what is wrong is the mixing up of equilibrium and non-equilibrium conditions by inserting cell (load) current into the Nernst voltage expression. It can be argued that expressing the Nernst voltage as a function of current is a "quick-and-dirty" trick that makes modeling easy for us. However, by taking such a shortcut, we compromise scientific rigor for the sake of practical convenience.

Conflicts of Interest: The author declares no conflict of interest.

Abbreviations

The following abbreviations are used in this manuscript:

SOFC	Solid oxide fuel cell
PEMFC	Proton exchange membrane fuel cell
EMF	Electromotive force
E_{Nernst}	Nernst potential (open-circuit EMF) of a single cell, V
E_0	Standard (reference) EMF of a single cell, V
E_0^0	Standard (reference) EMF of a single cell at temperature T_0, V
V	Output terminal voltage of a single cell, V
T	Temperature, K
n	Number of electrons transferred
a	Activity
a_{H_2}	Activity of hydrogen
a_{O_2}	Activity of oxygen
a_{H_2O}	Activity of water vapor (steam)
Δs	Change in entropy, J/(mol K)
p	Pressure or partial pressure, atm
p^0	Standard-state pressure, atm
p_{H_2}	Partial pressure of hydrogen, atm
p_{O_2}	Partial pressure of oxygen, atm
p_{H_2O}	Partial pressure of water vapor, atm
I_{FC}	Fuel cell current, A
u	Fuel utilization ratio
r_{HO}	Ratio of hydrogen-to-oxygen input flow rates
K_{H_2}	Valve molar constant for hydrogen, mol/(s atm)
K_{O_2}	Valve molar constant for oxygen, mol/(s atm)
K_{H_2O}	Valve molar constant for water vapor, mol/(s atm)
K_r	Modeling constant, mol/(s A)
V_{anode}	Anode compartment volume, m^3
$V_{cathode}$	Cathode compartment volume, m^3
t	Time, s
$n_{H_2}^{anode}$	Amount of hydrogen in the anode channel, mol
$q_{H_2}^{anode}$	Rate of change of the quantity of hydrogen in the anode channel, mol/s
$q_{H_2}^{in}$	Hydrogen input flow rate, mol/s
$q_{H_2}^{out}$	Hydrogen output flow rate, mol/s
$q_{H_2}^{react}$	Hydrogen flow rate that takes part in the reaction, mol/s
$q_{O_2}^{cathode}$	Rate of change of the amount of oxygen in the cathode channel, mol/s
$q_{O_2}^{in}$	Oxygen input flow rate, mol/s

$q_{O_2}^{out}$	Oxygen output flow rate, mol/s
$q_{O_2}^{react}$	Oxygen reacting flow rate, mol/s
$q_{H_2O}^{anode}$	Rate of change of the amount of water vapor in the anode channel, mol/s
$q_{H_2O}^{out}$	Water vapor output flow rate, mol/s
$q_{H_2O}^{react}$	Water vapor flow rate produced in the reaction, mol/s
τ_{H_2}	Hydrogen flow response time constant, s
τ_{O_2}	Oxygen flow response time constant, s
τ_{H_2O}	Water vapor flow response time constant, s
r	Ohmic resistance of a single cell, Ohm
ss	Notation (used in the subscript) to indicate steady-state values
$\mathcal{X}(s)$	Laplace transform of $x(t)$
R	Universal gas constant, J/(mol K)
F	Faraday's constant, Coulombs/mol

Appendix A

The intermediate steps in the derivations of Equations (8) and (33) are provided in this Appendix.

Appendix A.1. Equation (33)

At steady state, there are no changes in the input/output flow rates or the current, and the partial pressures of hydrogen, oxygen and water vapor have fixed (unchanging) values. Of course, corresponding to a load change, the cell (stack) may move from one fixed (steady) state to another fixed (steady) state. The steady-state partial pressure of a reactant or product can be obtained by setting the time derivative of its partial pressure to zero and solving for the partial pressure. From Equation (13), setting

$$\frac{d}{dt} p_{H_2}^{anode} = 0, \tag{A1}$$

we have at steady state

$$q_{H_2,ss}^{in} - q_{H_2,ss}^{react} - q_{H_2,ss}^{out} = 0 \tag{A2}$$

which, by Equations (17) and (22), becomes

$$q_{H_2,ss}^{in} - 2K_r I_{FC,ss} - K_{H_2} p_{H_2,ss} = 0, \tag{A3}$$

which, after rearrangement of terms, yields Equation (33).

Appendix A.2. Equation (8)

We will need the definitions of the fuel utilization ratio [2,6],

$$u = \frac{q_{H_2}^{react}}{q_{H_2}^{in}}, \tag{A4}$$

and the ratio of hydrogen-to-oxygen input flow rates [2,6]:

$$r_{HO} = \frac{q_{H_2}^{in}}{q_{O_2}^{in}}. \tag{A5}$$

Using Equations (33)–(35) (and omitting the steady-state subscript for simplicity), we have

$$\ln\left(\frac{p_{H_2}\sqrt{p_{O_2}}}{p_{H_2O}}\right) = \ln\left\{\frac{K_{H_2O}}{K_{H_2}}\left(\frac{q_{H_2}^{in}}{2K_rI_{FC}}-1\right)\sqrt{\frac{1}{K_{O_2}}(q_{O_2}^{in}-K_rI_{FC})}\right\} \tag{A6}$$

$$= \ln\left\{\frac{K_{H_2O}}{K_{H_2}}\left(\frac{1}{u}-1\right)\sqrt{\frac{1}{K_{O_2}}(q_{O_2}^{in}-K_rI_{FC})}\right\} \text{ from Equations (22) and (A4)} \tag{A7}$$

$$= \ln\left\{\frac{K_{H_2O}}{K_{H_2}}\left(\frac{1}{u}-1\right)\sqrt{\frac{1}{K_{O_2}}\left(\frac{q_{H_2}^{in}}{r_{HO}}-K_rI_{FC}\right)}\right\} \text{ from Equation (A5)} \tag{A8}$$

$$= \ln\left\{\frac{K_{H_2O}}{K_{H_2}}\left(\frac{1}{u}-1\right)\sqrt{\frac{1}{K_{O_2}}K_rI_{FC}\left(\frac{q_{H_2}^{in}}{r_{HO}K_rI_{FC}}-1\right)}\right\} \tag{A9}$$

$$= \ln\left\{\frac{K_{H_2O}}{K_{H_2}}\left(\frac{1}{u}-1\right)\sqrt{\frac{1}{r_{HO}K_{O_2}}K_rI_{FC}\left(\frac{q_{H_2}^{in}}{K_rI_{FC}}-r_{HO}\right)}\right\} \tag{A10}$$

$$= \ln\left\{\frac{K_{H_2O}}{K_{H_2}}\left(\frac{1}{u}-1\right)\sqrt{\frac{1}{r_{HO}K_{O_2}}K_rI_{FC}\left(\frac{2}{u}-r_{HO}\right)}\right\} \text{ from Equations (22) and (A4)} \tag{A11}$$

$$= \ln\left(\frac{K_{H_2O}}{K_{H_2}}\sqrt{\frac{K_r}{r_{HO}K_{O_2}}}\right) + \ln\left\{\left(\frac{1}{u}-1\right)\sqrt{I_{FC}\left(\frac{2}{u}-r_{HO}\right)}\right\} \tag{A12}$$

$$= \ln\left(\frac{K_{H_2O}}{K_{H_2}}\sqrt{\frac{K_r}{r_{HO}K_{O_2}}}\right) + \ln\left\{\sqrt{I_{FC}\left(\frac{1}{u}-1\right)^2\left(\frac{2}{u}-r_{HO}\right)}\right\} \tag{A13}$$

$$= \ln\left(\frac{K_{H_2O}}{K_{H_2}}\sqrt{\frac{K_r}{r_{HO}K_{O_2}}}\right) + \frac{1}{2}\ln\left\{I_{FC}\left(\frac{1}{u}-1\right)^2\left(\frac{2}{u}-r_{HO}\right)\right\} \tag{A14}$$

The derivation of Equation (8) is complete upon the substitution of Equation (A14) into Equation (6).

References

1. Padulles, J.; Ault, G.W.; McDonald, J.R. An integrated SOFC plant dynamic model for power systems simulation. *J. Power Sources* **2000**, *86*, 495–500. [CrossRef]
2. Zhu, Y.; Tomsovic, K. Development of models for analyzing the load-following performance of microturbines and fuel cells. *Electr. Power Syst. Res.* **2002**, *62*, 1–11. [CrossRef]
3. El-Sharkh, M.Y.; Rahman, A.; Alam, M.S.; Byrne, P.C.; Sakla, A.A.; Thomas, T. A dynamic model for a stand-alone PEM fuel cell power plant for residential applications. *J. Power Sources* **2004**, *138*, 199–204. [CrossRef]
4. Jurado, F.; Valverde, M. Multiobjective genetic algorithms for fuzzy inverter in solid oxide fuel cell system. In Proceedings of the IEEE International Symposium on Industrial Electronics (ISIE), Dubrovnik, Croatia, 20–23 June 2005.
5. Jurado, F.; Valverde, M. Genetic fuzzy control applied to the inverter of solid oxide fuel cell for power quality improvement. *Electr. Power Syst. Res.* **2005**, *76*, 93–105. [CrossRef]
6. Li, Y.H.; Choi, S.S.; Rajakaruna, S. An analysis of the control and operation of a solid oxide fuel-cell power plant in an isolated system. *IEEE Trans. Energy Convers.* **2005**, *20*, 381–387. [CrossRef]
7. Li, Y.H.; Rajakaruna, S.; Choi, S.S. Control of a solid oxide fuel cell power plant in a grid-connected system. *IEEE Trans. Energy Convers.* **2007**, *22*, 405–413. [CrossRef]
8. Wang, C.; Nehrir, M.H.; Shaw, S.R. Dynamic models and model validation for PEM fuel cells using electrical circuits. *IEEE Trans. Energy Convers.* **2005**, *20*, 442–451. [CrossRef]
9. Wang, C.; Nehrir, M.H. A physically based dynamic model for solid oxide fuel cells. *IEEE Trans. Energy Convers.* **2007**, *22*, 887–897. [CrossRef]
10. Huo, H.-B.; Zhong, Z.-D.; Zhu, X.-J.; Tu, H.-Y. Nonlinear dynamic modeling for a SOFC stack by using a Hammerstein model. *J. Power Sources* **2008**, *175*, 441–446. [CrossRef]
11. Wu, X.-J.; Zhu, X.-J.; Cao, G.-Y.; Tu, H.-Y. Predictive control of SOFC based on a GA-RBF neural network. *J. Power Sources* **2008**, *179*, 232–239. [CrossRef]

12. Chakraborty, U.K. Static and dynamic modeling of solid oxide fuel cell using genetic programming. *Energy* **2009**, *34*, 740–751. [CrossRef]

13. Chakraborty, U.K. An error in solid oxide fuel cell stack modeling. *Energy* **2011**, *36*, 801–802. [CrossRef]

14. Nayeripour, M.; Hoseintabar, M.; Niknam, T. A new method for dynamic performance improvement of a hybrid power system by coordination of converter's controller. *J. Power Sources* **2011**, *196*, 4033–4043. [CrossRef]

15. Nayeripour, M.; Hoseintabar, M.; Niknam, T.; Adabi, J. Power management, dynamic modeling and control of wind/FC/battery-bank based hybrid power generation system for stand-alone application. *Eur. Trans. Electr. Power* **2012**, *22*, 271–293. [CrossRef]

16. Radisavljevic, V. On controllability and system constraints of the linear models of proton exchange membrane and solid oxide fuel cells. *J. Power Sources* **2011**, *196*, 8549–8552. [CrossRef]

17. Torreglosa, J.P.; García, P.; Fernández, L.M.; Jurado, F. Predictive control for the energy management of a fuel-cell–battery–supercapacitor tramway. *IEEE Trans. Ind. Inform.* **2014**, *10*, 276–285. [CrossRef]

18. Fedakar, S.; Bahceci, S.; Yalcinoz, T. Modeling and simulation of grid connected solid oxide fuel cell using PSCAD. *J. Renew. Sustain. Energy* **2014**, *6*, 053118. [CrossRef]

19. Taghizadeh, M.; Hoseintabar, M.; Faiz, J. Frequency control of isolated WT/PV/SOFC/UC network with new control strategy for improving SOFC dynamic response. *Int. Trans. Electr. Energy Syst.* **2015**, *25*, 1748–1770. [CrossRef]

20. Chettibi, N.; Mellit, A.; Sulligoi, G.; Massi Pavan, A. Fuzzy-based power control for distributed generators based on solid oxide fuel cells. In Proceedings of the IEEE International Conference on Clean Electrical Power (ICCEP), Taormina, Italy, 16–18 June 2015; pp. 580–585. [CrossRef]

21. Barelli, L.; Bidini, G.; Ottaviano, A. Solid oxide fuel cell modelling: Electrochemical performance and thermal management during load-following operation. *Energy* **2016**, *115*, 107–119. [CrossRef]

22. Vigneysh, T.; Kumarappan, N. Autonomous operation and control of photovoltaic/solid oxide fuel cell/battery energy storage based microgrid using fuzzy logic controller. *Int. J. Hydrogen Energy* **2016**, *41*, 1877–1891. [CrossRef]

23. Wu, Z.; Shi, W.; Li, D.; He, T.; Xue, Y.; Han, M.; Zheng, S. The disturbance rejection design based on physical feedforward for solid oxide fuel cell. In Proceedings of the 17th IEEE International Conference on Control, Automation and Systems (ICCAS), Jeju, Korea, 18–21 October 2017.

24. Pan, L.; Xue, Y.; Sun, L.; Li, D.; Wu, Z. Multiple model predictive control for solid oxide fuel cells. In Proceedings of the ASME 2017 International Design Engineering Technical Conferences and Computers and Information in Engineering Conference (IDETC/CIE 2017), Cleveland, OH, USA, 6–9 August 2017.

25. Wu, G.; Sun, L.; Lee, K.Y. Disturbance rejection control of a fuel cell power plant in a grid-connected system. *Control Eng. Pract.* **2017**, *60*, 183–192. [CrossRef]

26. Sun, L.; Hua, Q.; Shen, J.; Xue, Y.; Li, D.; Lee, K.Y. A combined voltage control strategy for fuel cell. *Sustainability* **2017**, *9*, 1517. [CrossRef]

27. Darjat; Sulistyo; Triwiyatno, A.; Thalib, H. The design of connection solid oxide fuel cell (SOFC) integrated grid with three-phase inverter. *IOP Conf. Ser. Mater. Sci. Eng.* **2018**, *316*, 012057. [CrossRef]

28. Sun, L.; Wu, G.; Xue, Y.; Shen, J.; Li, D.; Lee, K.Y. Coordinated control strategies for fuel cell power plant in a microgrid. *IEEE Trans. Energy Convers.* **2018**, *33*, 1–9. [CrossRef]

29. Chettibi, N.; Mellit, A. Intelligent control strategy for a grid connected PV/SOFC/BESS energy generation system. *Energy* **2018**, *147*, 239–262. [CrossRef]

30. Safari, A.; Shahsavari, H.; Salehi, J. A mathematical model of SOFC power plant for dynamic simulation of multi-machine power systems. *Energy* **2018**, *149*, 397–413. [CrossRef]

31. Larminie, J.; Dicks, A. *Fuel Cell Systems Explained*, 2nd ed.; Wiley: Chichester, UK, 2003.

32. Udagawa, J.; Aguiar, P.; Brandon, N.P. Hydrogen production through steam electrolysis: Model-based steady state performance of a cathode-supported intermediate temperature solid oxide electrolysis cell. *J. Power Sources* **2007**, *166*, 127–136. [CrossRef]

33. Chakraborty, U.K.; Abbott, T.; Das, S.K. PEM fuel cell modeling using differential evolution. *Energy* **2012**, *40*, 387–399. [CrossRef]